united nations
educational, scientific
and cultural
organization

international atomic
energy agency

the
abdus salam
international centre for theoretical physics

School on "Exploring the Atmosphere by Remote Sensing Techniques"
18 October - 5 November 1999

1151-3

"Improved Mie Scattering Algorithms"

&

"Efficiency Factors in Mei Scattering"

W. Wisombe
NASA/GCFC
Greenbelt, MD
USA

Reprinted from **Applied Optics**, Vol. 19, page 1505, May 1, 1980

Improved Mie scattering algorithms

W. J. Wiscombe

Scattering of electromagnetic radiation from a sphere, so-called Mie scattering, requires calculations that can become lengthy and even impossible for those with limited resources. At the same time, such calculations are required for the widest variety of optical applications, extending from the shortest UV to the longest microwave and radar wavelengths. This paper briefly describes new and thoroughly documented Mie scattering algorithms that result in considerable improvements in speed by employing more efficient formulations and vector structure. The algorithms are particularly fast on the Cray-1 and similar vector-processing computers.

I. Introduction

Mie scattering calculations pervade the entire field of atmospheric optics. Applications range from one end of the electromagnetic spectrum to the other—from UV solar radiation backscattered by stratospheric aerosols to satellites, through visible and IR radiation scattered by clouds and aerosols, to microwaves and radar scattered from large hydrometeors.

The actual formulas for Mie scattering are well known.[1,2] The quantities required are

$$Q_{\text{ext}} = \frac{2}{x^2}\sum_{n=1}^{N}(2n+1)\text{Re}(a_n + b_n), \tag{1a}$$

$$Q_{\text{sca}} = \frac{2}{x^2}\sum_{n=1}^{N}(2n+1)(|a_n|^2 + |b_n|^2), \tag{1b}$$

$$g = \frac{4}{x^2 Q_{\text{sca}}}\sum_{n=1}^{N}\left[\frac{n(n+2)}{n+1}\text{Re}(a_n a_{n+1}^* + b_n b_{n+1}^*) + \frac{2n+1}{n(n+1)}\text{Re}(a_n b_n^*)\right], \tag{1c}$$

$$S_1(\mu) = \sum_{n=1}^{N}\frac{2n+1}{n(n+1)}[a_n\pi_n(\mu) + b_n\tau_n(\mu)], \tag{1d}$$

$$S_2(\mu) = \sum_{n=1}^{N}\frac{2n+1}{n(n+1)}[a_n\tau_n(\mu) + b_n\pi_n(\mu)], \tag{1e}$$

which are, respectively, the extinction efficiency, scattering efficiency, asymmetry factor, and complex scattering amplitudes for two orthogonal directions of incident polarization. ($|S_1|^2$ and $|S_2|^2$ are the scattered intensities.) Size parameter x is the sphere's circumference divided by the wavelength. The complex-valued Mie coefficients a_n and b_n depend on x and on the complex refractive index $m = m_{\text{Re}} - im_{\text{Im}}$. They are expressed in terms of spherical Bessel functions; in particular, following Infeld's formulation,[3] they involve the function

$$A_n(mx) = \psi_n'(mx)/\psi_n(mx), \tag{2}$$

where $\psi_n(z) \equiv zj_n(z)$. Finally, μ is the cosine of the scattering angle, and the angular eigenfunctions are

$$\pi_n(\mu) = P_n'(\mu), \tag{3}$$

$$\tau_n(\mu) = \mu\pi_n(\mu) - (1-\mu^2)\pi_n'(\mu), \tag{4}$$

where P_n is a Legendre polynomial.

The only remaining question is how to structure the Mie computation for maximum efficiency, while at the same time maintaining accuracy and avoiding numerical instability and ill-conditioning. The first published Mie algorithms were those of Dave[4,5] although Irvine, Plass, and Cheyney, to name just a few, had been doing Mie calculations for several years prior. Most new investigators in the intervening years tended to use Dave's algorithms or variants thereof.

Mie calculations have gained a reputation for being time-consuming. This is, first, because the upper limit N in Eqs. (1) is roughly equal to x, which can become very large, e.g., about 1260 for a 100-μm water drop at a visible wavelength of 0.5 μm. Second, because in typical applications one wishes to sum these series for a large number of radii (as in integrating over a size distribution) or for a large number of wavelengths (as in integrating across the solar spectrum) or for a large number of refractive indices (as in inverting scattering measurements to deduce refractive index). The present author alone has used many hours of Univac 1108, IBM 360/91, CDC 7600, and Cray-1 time doing Mie computations.

The author is with National Center for Atmospheric Research, Boulder, Colorado 80307.

Received 12 December 1979.
0003-6935/80/091505-05$00.50/0.

In light of all this, it seems likely that a pair of new and very efficient Mie algorithms, which the author has developed over the past several years and which are fully described in a recent report,[6] will be of broad interest. A synopsis of the original features of the algorithms and certain selected timing comparisons are given below. For the remaining features and listings of computer codes implementing the algorithms, the reader is referred to the report cited in Ref. 6.

II. A_n Computation

The complex function A_n was computed by upward recurrence in the early days of Mie calculations. Then Kattawar and Plass[7] showed that upward recurrence could be highly unstable if absorption (m_{Im}) was large enough, but that downward recurrence was always stable. Dave[4] allowed for this by furnishing two algorithms, one with upward recurrence and one with downward recurrence; the user could take his pick.

This seemed a highly unsatisfactory state in which to leave the matter. Therefore we sought a criterion for determining *a priori*, from x and m, when down recurrence had to be used (when it is safe, up recurrence is always preferable because it is faster). At first we did this by observing the breakdown of many upward recursive A_n computations, from which we were able to descry an empirical criterion for allowing up recurrence. This had the form

$$m_{\mathrm{Im}}x \leq f(m_{\mathrm{Re}}). \tag{5}$$

Taking $f(m_{\mathrm{Re}})$ as linear in m_{Re} was not unreasonable, but we were able to make a much sharper determination.

We did this by not considering A_n computations in isolation, but by considering the full Mie computations. Exact Mie results were generated using down recurrence for A_n and compared with the corresponding results produced by up recurrence. At first we looked only at the Mie quantities Q_{ext}, Q_{sca}, and g [Eqs. (1a)–(1c)], and we counted up recurrence of A_n as a failure whenever it produced a relative error exceeding 10^{-6} in any one of these quantities. It was clear from our initial studies that for fixed x and m_{Re}, whenever up recurrence failed for a given imaginary index, it failed for all larger indices as well. Therefore, for each pair (x,m_{Re}) we performed an upward search on m_{Im} to find the first value m^*_{Im} at which up recurrence failed. The search was successively refined until m^*_{Im} was determined to 3 significant digits. We considered values of x from 1 to 10,000 and values of m_{Re} from 1.05 to 9.25, which should cover almost any conceivable situation of practical interest.

This search revealed that, for fixed m_{Re}, the product $m^*_{\mathrm{Im}}x$ rapidly approached an asymptotic value from above as x increased. This asymptotic value depended on m_{Re}. Mathematically speaking, this meant there was some function $f(m_{\mathrm{Re}})$ such that

$$xm^*_{\mathrm{Im}} \geq \min_{\text{all } x}(xm^*_{\mathrm{Im}}) \equiv f(m_{\mathrm{Re}}),$$

and such that the inequality was roughly an equality over almost the entire range of x. The values we obtained for $f(m_{\mathrm{Re}})$ are plotted as solid dots in Fig. 1(a). They can be fitted quite excellently by the polynomial expression

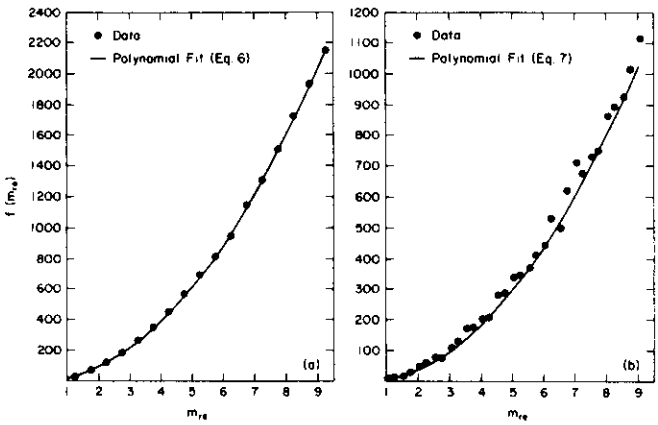

Fig. 1. Empirically determined values for the function $f(m_{\mathrm{Re}})$ described in the text, and polynomical fits to those data: (a) considers Q_{ext}, Q_{sca}, and g only; (b) includes the angular functions S_1 and S_2 as well.

$$f_1(m_{\mathrm{Re}}) \equiv -8 + 26.22m^2_{\mathrm{Re}} - 0.4474m^3_{\mathrm{Re}} + 0.00204m^6_{\mathrm{Re}} - 0.000175m^7_{\mathrm{Re}}, \tag{6}$$

which lies on or slightly under most of the data points. [A quadratic in m_{Re} gives an acceptable fit, but Eq. (6) is considerably better.]

We then extended our study to include the angular scattering functions S_1 and S_2 [Eqs. (1d) and (1e)], calculated at 1° increments from 0° to 180° inclusive. Up recurrence was regarded as a failure if at any angle the real or imaginary part of S_1 or S_2 had a relative error exceeding 10^{-5}. (Q_{ext}, Q_{sca}, and g played no role because their relative errors were invariably down at the 10^{-10} level when S_1 or S_2 relative errors first reached 10^{-5}. The reason is that the earlier terms in the S_1 or S_2 sums may cancel, so that the later terms, which are most sensitive to up-recurrence instability, dominate the sum; this phenomenon is greatly mitigated in the sums for Q_{ext}, Q_{sca}, and g.) The data we obtained are plotted in Fig. 1(b). They are considerably more noisy than the data in Fig. 1(a), which is due to the following circumstance: sometimes the real part of S_1 or S_2 is orders of magnitude smaller than the imaginary part or vice versa. These very small components are quite sensitive to up-recurrence errors because considerable cancellation of significant digits has taken place in summing for them. These very small components, which dominate the $f(m_{\mathrm{Re}})$ determination, are necessarily noisier than Q_{ext}, Q_{sca}, or g. Because the data in Fig. 1(b) are more erratic than they are in Fig. 1(a), we have only fitted a quadratic to them:

$$f_2(m_{\mathrm{Re}}) = 13.78m^2_{\mathrm{Re}} - 10.8m_{\mathrm{Re}} + 3.9. \tag{7}$$

This function was chosen to lie under almost all the data points in order to be conservative.

A more limited study than the present one was done by Wiscombe.[6] The scattered intensity $|S_1|^2 + |S_2|^2$ and the degree of polarization $(|S_2|^2 - |S_1|^2)/(|S_2|^2 +$

Table I. Comparison of Number of Iterations Required by the Dave and Lentz Methods to Calculate $A_N(mx)$ in Situations Where Eq. (7) Requires Down Recurrence[a]

x	m	Number of iterations: Dave method	Number of iterations: Lentz method
100	$1.05 - i$	41	16
	$1.50 - i$	80	22
	$1.95 - i$	122	31
1000	$1.05 - 0.01i$	115	53
	$1.05 - 0.1i$	121	32
	$1.05 - i$	555	20
	$1.50 - 0.1i$	613	135
	$1.50 - i$	943	28
	$1.95 - 0.1i$	1,108	254
	$1.95 - i$	1,370	42
10,000	$1.05 - 0.01i$	1,464	232
	$1.05 - 0.1i$	1,519	40
	$1.05 - i$	5,864	20
	$1.50 - 0.01i$	6,414	1384
	$1.50 - 0.1i$	6,447	161
	$1.50 - i$	9,747	30
	$1.95 - 0.01i$	11,364	2599
	$1.95 - 0.1i$	11,392	309
	$1.95 - i$	14,020	44

[a] A convergence criterion of 10^{-8} was used in the Lentz method.

$|S_1|^2$) were examined at 60 angles rather than S_1 and S_2 at 181 angles, and m_{Re} was varied only from 1.05 to 2.5. The criterion so derived was

$$f_3(m_{\mathrm{Re}}) = 16.35m_{\mathrm{Re}}^2 + 8.42m_{\mathrm{Re}} - 15.04, \quad (8)$$

which falls roughly midway between $f_1(m_{\mathrm{Re}})$ and $f_2(m_{\mathrm{Re}})$.

Equation (5)–(7) furnish *a priori* criteria when up recurrence of A_n is safe. If down recurrence must be used, it can be made considerably more efficient by initializing it using the Lentz method[8] rather than using Dave's method.[5] Dave initializes using $A_N^*(mx) = 0$, where $N^* = 1.1|mx| + 1$. Presuming $N^* > N \simeq x + 4x^{1/3} + 1$ (see Sec. V) and since only A_1 through A_N are required, Dave's method requires about $(1.1|m| - 1)x - 4x^{1/3}$ iterations to get A_N. (We say presuming because we have found many cases where $N^* < N$, so that Dave's method fails utterly. For example, $N^* = 17$ while $N = 19$ for $m = 1.05 - i$ and $x = 10$; or $N^* = 117$ while $N = 119$ for $m = 1.05 - 0.1i$ and $x = 100$.) Table I compares this number, for a few values of m and x not satisfying Eq. (5), with the number of Lentz method iterations necessary to calculate A_N. Since an iteration of either type requires about the same amount of computation time, the Lentz method clearly enjoys a dramatic advantage. The number of Dave iterations furthermore rises sharply as the imaginary index increases, while the number of Lentz iterations falls in the same situation. The Lentz method also has an error that is easily controllable and has explicit procedures to avoid ill-conditioning.

It should be emphasized that the Lentz method is only faster in combination with our up-recurrence criterion. A more extensive version of Table I (see Ref. 6) shows that, as the imaginary index falls below m_{Im}^*, the number of Lentz method iterations rises sharply and becomes comparable with the number of Dave method iterations.

The above empirical criteria are, of course, somewhat dependent on computer precision. On the CDC and Cray-1 machines all computations could be done in single precision (14 significant digits). But the 8 significant digit single precision on the IBM and Univac machines is inadequate, and one must do the A_n recurrence (but not the A_N initialization for down recurrence) in double precision on those machines.

III. S_1 and S_2 Computation

The computation of scattering amplitudes S_1 and S_2 [Eqs. (1d) and (1e)] ordinarily requires almost all the time in a Mie scattering calculation. This is because the right-hand sides in Eqs. (1d) and (1e) are typically summed for many angles. Thus efficiency in this part of the calculation is mandatory. We achieve this efficiency partly by vector structure (see Sec. VI) and partly by two devices to be discussed in this section.

First, we have derived more efficient recurrences for the angular eigenfunctions π_n and τ_n [Eqs. (3) and (4)], namely,

$$\tau_n(\mu) = nt - \pi_{n-1}(\mu),$$

$$\pi_{n+1}(\mu) = s + \left(\frac{n+1}{n}\right)t,$$

where $s \equiv \mu\pi_n(\mu)$, and $t \equiv s - \pi_{n-1}(\mu)$. Derivations are given in Ref. 6. These recurrences require a total of three multiplications and three additions, compared with six multiplications and four additions for Dave's recurrences.[5] [We have assumed precalculation of purely numerical factors like $(n + 1)/n$ in both cases.] In our scheme, $\tau_n(\mu)$ is calculated just before the nth series term is formed, while $\pi_{n+1}(\mu)$ is calculated just afterward; this allows the sharing of the common quantity t.

The second device consists in calculating not S_1 and S_2 but rather

$$S^+ \equiv S_1 + S_2 = \sum_{n=1}^{N} \frac{2n+1}{n(n+1)}(a_n + b_n)(\pi_n + \tau_n),$$

$$S^- \equiv S_1 - S_2 = \sum_{n=1}^{N} \frac{2n+1}{n(n+1)}(a_n - b_n)(\pi_n - \tau_n).$$

Assume that the purely numerical factor $(2n + 1)/n(n + 1)$ is incorporated into a_n and b_n *or* $a_n \pm b_n$ outside of the vector loops over angle where the S_1 and S_2 or $S^\pm$ series are incremented (see Sec. VI). Then only one multiplication and one addition are necessary to form a series term for S^+ or S^-, while two multiplications and one addition are required to form a series term for S_1 or S_2. After summing is completed, S_1 and S_2 are easily recaptured from $S^\pm$ at insignificant cost compared with the rest of the Mie calculation.

IV. Small Particle Approximation

In the small particle or Rayleigh limit $x \to 0$, the Mie formulas become ill-conditioned. In particular, the recurrence for A_n, the recurrence for a spherical Bessel function involved in a_n and b_n, and the numerator in

the expression for b_n, all involve subtraction of nearly equal numbers as $x \to 0$. After finding the usual formulas for this limit (e.g., those cited in Refs. 1 and 2) insufficiently accurate in cases where $m_{\mathrm{Im}} \ll 1$, as described by Wiscombe,[6] we developed improved versions as follows:

$$Q_{\mathrm{ext}} = 6x\ \mathrm{Re}\left(\hat{a}_1 + \hat{b}_1 + \frac{5}{3}\hat{a}_2\right),$$

$$Q_{\mathrm{sca}} = 6x^4 T,$$

$$g = \frac{1}{T}\mathrm{Re}[\hat{a}_1(\hat{a}_2 + \hat{b}_1)^*],$$

$$S_1(\mu) = \frac{3}{2}x^3\left[\hat{a}_1 + \left(\hat{b}_1 + \frac{5}{3}\hat{a}_2\right)\mu\right],$$

$$S_2(\mu) = \frac{3}{2}x^3\left[\hat{b}_1 + \hat{a}_1\mu + \frac{5}{3}\hat{a}_2(2\mu^2 - 1)\right],$$

where

$$T \equiv |\hat{a}_1|^2 + |\hat{b}_1|^2 + \frac{5}{3}|\hat{a}_2|^2,$$

$$\hat{a}_1 = 2i\frac{m^2-1}{3}\frac{1 - \frac{1}{10}x^2 + \frac{4m^2+5}{1400}x^4}{D},$$

$$D = m^2 + 2 + \left(1 - \frac{7}{10}m^2\right)x^2 - \frac{8m^4 - 385m^2 + 350}{1400}x^4 + 2i\frac{m^2-1}{3}x^3\left(1 - \frac{1}{10}x^2\right),$$

$$\hat{b}_1 = ix^2\frac{m^2-1}{45}\frac{1 + \frac{2m^2-5}{70}x^2}{1 - \frac{2m^2-5}{30}x^2},$$

$$\hat{a}_2 = ix^2\frac{m^2-1}{15}\frac{1 - \frac{1}{14}x^2}{2m^2 + 3 - \frac{2m^2-7}{14}x^2}.$$

This formulation retains 6 significant digits (compared with exact Mie results) up to $x = 0.1$, 4–5 digits up to $x = 0.2$, and 2–3 digits up to $x = 0.5$, provided $|m| \leq 2$. It loses accuracy as $|m|$ increases, so these formulas are used only when $|m|x \leq 0.1$, which ensures at least 6-digit accuracy.

V. Number of Terms in Mie Series

To take advantage of vector structure, one must estimate *a priori* the number of terms N in the Mie series [Eqs. (1a)–(1e)]. This is in direct contrast to Dave's procedure,[5] which consists in stopping summation when $|a_n|^2 + |b_n|^2$ falls below 10^{-14}. Analysis of the convergence behavior of these series reveals that it is only slightly influenced by refractive index and that $N \sim x$. In order to get a more precise estimate, we followed the suggestion of Khare[9] that $N \sim x + cx^{1/3}$, where the $x^{1/3}$ term accounts for edge wave contributions. Upon generating a large amount of data on N as a function of x using a convergence criterion like Dave's, we found that these data could be excellently fit by

$$N = \begin{cases} x + 4x^{1/3} + 1 & 0.02 \leq x \leq 8 \\ x + 4.05x^{1/3} + 2 & 8 < x < 4200 \\ x + 4x^{1/3} + 2 & 4200 \leq x \leq 20{,}000. \end{cases}$$

(Chýlek in a private communication noted that N must be taken roughly 1% higher than our value for the very special purpose of finding certain very narrow, very sharp spikes in Q_{ext}, etc., as a function of x. These spikes are actually observed in experiments employing single spheres suspended by laser light pressure.) This fit rarely overestimates the number of series terms required by more than one or two. And it applies to all refractive indices since Mie series convergence is determined entirely by Bessel functions of x alone.

VI. Vector Structure

The newer computers, like the Cray-1, process vectors in very much the same way that older machines processed scalars (see Ref. 10). This can lead to dramatic speed increases when calculations are structured to enable processing of entire vectors at once.

Mie calculations involve two types of vectors, one type having the index n in Eqs. (1a)–(1e) and one type having an angular index. Loops over index n can be completely vectorized except when summing is being done, in which case they are only partly vectorizable. But loops over angle are always fully vectorizable. Therefore, the angular loop for S_1 and S_2 is placed inside the summing loop, in order to achieve maximum vector structure; this explains the importance of the S_1 and S_2 calculation improvements in Sec. III.

The only significant parts of the Mie calculation which cannot be vector structured are the Lentz method for A_N and the recurrences for A_n and a certain spherical Bessel function. All such iterative computations, in which a result depends on one or more prior results, are intrinsically unvectorizable. But the remaining parts of the Mie calculation have been vectorized, including summing operations (using the techniques described by Johnson[10]).

VII. Timing Studies

Table II compares published times for Dave's algorithms[4] and the faster of the two algorithms in the Wiscombe report.[6] (The slower algorithm is designed to use the absolute minimum amount of memory, which

Table II. Execution Times for Dave[5] and Wiscombe[6] Algorithms for a Single Mie Calculation [Eqs. (1a)–(1e)] with 182 Scattering Angles[a]

	Time (sec)	
x	Dave[5]	Wiscombe[6]
0.1	0.7	0.00018
1	1.1	0.00036
10	3.7	0.00098
100	22	0.0054
1000	194	0.0456
5000	945	0.222

[a] Dave used an IBM 360/50, which is about 100 times slower than the Cray-1 used by Wiscombe.

Table III. Cray-1 Times (in Milliseconds) to Execute the Vectorized MIEV1 Code[6] for Various Combinations of Mie Size Parameters and Number of Angles[a]

No. of angles	Mie size parameter							
	1	3.3	10	33	100	333	1000	5000
0	0.083	0.10	0.14	0.25	0.53	1.5	5.6	21
3	0.13	0.18	0.28	0.57	1.3	3.8	12	53
7	0.13	0.18	0.29	0.59	1.4	4.0	13	55
15	0.14	0.20	0.32	0.66	1.5	4.5	14	62
31	0.16	0.23	0.39	0.80	1.9	5.5	17	77
63	0.20	0.29	0.51	1.1	2.6	7.7	23	106
127	0.29	0.42	0.75	1.6	4.0	12	35	165
255	0.47	0.73	1.3	2.9	7.2	22	63	298

[a] Each time represents an average over $m_{\mathrm{Re}} = 1.1(0.2)2.5$, with $m_{\mathrm{Im}} = 0.1$.

exacts a penalty of lesser efficiency.) The new algorithm is 30–40 times faster when the difference in basic computer speed is factored out. Of this, a factor of ~7 is due to the vector structure, a factor of ~2 to more efficient formulations, and the remaining improvement to the use of single precision rather than the slower double precision of Dave's routines.

Table III shows the times required to do Mie calculations with the new algorithm, for size parameters ranging from 1 to 5000 and anywhere from 0 to 255 scattering angles. Each quoted time is an average over the times for eight values of m_{Re} for fixed $m_{\mathrm{Im}} = 0.1$. [The times are 5–30% faster for $m_{\mathrm{Im}} = 0$ because special branches are taken in the Mie coefficient (a_n,b_n) calculation and because only up recurrence is used for A_n.]

There is a big rise, a factor of 2–3, in going from zero to three angles in Table III. But after this initial jump, one must go all the way to sixty-three angles to double the three-angle time. This shows the dramatic advantage of vectorized angular loops, as well as the savings to be reaped if only Q_{ext}, Q_{sca}, and g are required.

For size parameters x below 100, the Table III times rise considerably more slowly than linearly in x, demonstrating the advantage of vector structure in certain n loops, including the ones for summing. Only beyond $x = 100$ do the times go up about linearly in x, but this phenomenon is specific to the Cray-1 and comes about because the Cray-1 processes vectors in sixty-four-element segments.

Timing studies like these furnish a concrete basis for testing claims of Mie algorithm improvement and incidentally allow one to make rough *a priori* estimates of the times required for particular Mie computations.

VIII. Summary

Dramatically faster Mie algorithms have been made possible by vector structuring and by much more efficient handling of the A_n and S_1 and S_2 calculations. Better formulas for the small particle case are also presented. Timing studies indicate a factor of 30–40 improvement over Dave's algorithms[4] when intermachine differences are removed. Accuracy of the new algorithms is 5–6 significant digits or better, and they have been used without difficulty up to size parameters of 20,000 for real refractive indices from 1 to 9 and imaginary indices from 0 to 10. Mie calculations which were impossibly long a few years ago can be done routinely with these algorithms.

We thank Ron Welch (University of Mainz, Germany) and Eric Smith (Colorado State University) for encouraging us to make these algorithms more widely available and Tom Ackerman (NASA Ames) for testing the slower one (MIEV0) directly against Dave's DBMIE (converted to single precision) on his CDC 7600.

The National Center for Atmospheric Research is sponsored by the National Science Foundation.

References

1. H. C. Van de Hulst, *Light Scattering by Small Particles* (Wiley, New York, 1957).
2. M. Kerker, *The Scattering of Light and Other Electromagnetic Radiation* (Academic, New York, 1969).
3. L. Infeld, Q. Appl. Math. **5**, 113 (1947).
4. J. V. Dave, "Subroutines for Computing the Parameters of the Electromagnetic Radiation Scattered by a Sphere," Report 320-3237 (IBM Scientific Center, Palo Alto, Calif., 1968).
5. J. V. Dave, IBM J. Res. Dev. **13**, 302 (1969).
6. W. J. Wiscombe, "Mie Scattering Calculations: Advances in Technique and Fast, Vector-Speed Computer Codes," NCAR Technical Note NCAR/TN-140+STR (National Center for Atmospheric Research, Boulder, Colo. 80307, 1979).
7. G. W. Kattawar and G. N. Plass, Appl. Opt. **6**, 1377 (1967).
8. W. J. Lentz, Appl. Opt. **15**, 668 (1976).
9. V. Khare, "Short-Wavelength Scattering of Electromagnetic Waves by a Homogeneous Dielectric Sphere," Ph.D. Thesis, U. Rochester, N.Y., 1976 (available from University Microfilms, Ann Arbor, Mich.).
10. P. M. Johnson, Comput. Des. **17**, 89 (1978).

Efficiency Factors in Mie Scattering

H. M. Nussenzveig[a]
Cooperative Institute for Research in the Environmental Sciences, Boulder, Colorado 80309, and National Center for Atmospheric Research, Boulder, Colorado 80307

and

W. J. Wiscombe
National Center for Atmospheric Research, Boulder, Colorado 80307

(Received 22 May 1980)

Asymptotic approximations to the Mie efficiency factors for extinction, absorption, and radiation pressure, derived from complex-angular-momentum theory and averaged over $\Delta\beta \sim \pi$ (β = size parameter), are given and compared with the exact results. For complex refractive indices $N = n + i\kappa$ with $1.1 \leq n \leq 2.5$ and $0 \leq \kappa \leq 1$, the relative errors decrease from $\sim(1\text{–}10)\%$ to $\sim(10^{-2}\text{–}10^{-3})\%$ between $\beta = 10$ and $\beta = 1000$, and computing time is reduced by a factor of order β, so that the Mie formulae can advantageously be replaced by the asymptotic ones in most applications.

PACS numbers: 42.20.Gg, 42.68.Vs

The Mie efficiency factors[1] for extinction (Q_{ext}), absorption (Q_{abs}), and radiation pressure (Q_{pr}) are just the corresponding cross sections divided by the projected area πa^2 of the scattering sphere. These quantities are important in many applications. Typical size parameters $\beta = ka$ (k = wave number, a = droplet radius) range from $\ll 1$ up to $\sim 10^4$, with complex refractive indices $N = n + i\kappa$, $1.1 \lesssim n \lesssim 1.9$, $10^{-8} \lesssim \kappa \lesssim 1$. The efficiencies vary extremely rapidly[2] with β, n and κ; but in most applications one is only interested in means $\langle Q \rangle$ over some range $\Delta\beta$, not in this high-frequency "ripple."

Evaluation of the exact Mie expressions[1] requires summing $\sim \beta$ partial waves. Upon integration across size or wavelength with a step fine enough to resolve the ripple ($\Delta\beta \leq 0.01\text{–}0.1$), one is faced with exorbitant computation times. Approximations[1] based on geometrical optics and classical diffraction theory do not have the required accuracy until β exceeds several thousand (cf. below). Clearly, better approximations, devoid of ripple, are needed.

The complex-angular-momentum theory of Mie scattering[3] can furnish such approximations. By a simple extension of previously developed tech-

niques,[4,5] we find for the extinction efficiency,

$$Q_{ext} = 2 + 1.992\,386\,1\beta^{-2/3} + 8\,\mathrm{Im}\left\{\tfrac{1}{4}(N^2+1)(N^2-1)^{-1/2}\beta^{-1} - N^2(N+1)^{-1}(N^2-1)^{-1}\left[1+\frac{i}{2\beta}\left(\frac{1}{N-1}-\frac{N-1}{N}\right)\right]\beta^{-1}\right.$$
$$\times\exp[2i(N-1)\beta] - \tfrac{1}{2}(N-1)\sum_{j=1}^{\infty}\left[j-\left(\frac{N-1}{2}\right)\right]^{-1}\left(\frac{N-1}{N+1}\right)^{2j}$$
$$\left.\times\exp[2i(N-1+2jN)\beta]\right\} - 0.715\,353\,7\beta^{-4/3} - 0.332\,064\,3$$
$$\times\mathrm{Im}[e^{i\pi/3}(N^2-1)^{-3/2}(N^2+1)(2N^4-6N^2+3)]\beta^{-5/3} + O(\beta^{-2}) + \text{ripple}. \quad (1)$$

To obtain the average absorption efficiency $\langle Q_{abs}\rangle$ over $\Delta\beta \sim \pi$, one applies the modified Watson transformation[3] to the corresponding Mie series expansion[1,2] and then takes the average over $\Delta\beta$. The result[6] is

$$\langle Q_{abs}\rangle = \langle Q_{abs}\rangle_F + \langle Q_{abs}\rangle_{a.e.} + \langle Q_{abs}\rangle_{b.e.}, \quad (2)$$

$$\langle Q_{abs}\rangle_F = \sum_{\lambda=1}^{2}\int_0^{\pi/2}\varphi(r_{j\lambda})\sin\theta\cos\theta\,d\theta, \quad (3)$$

$$\langle Q_{abs}\rangle_{a.e.} = 2^{-1/3}\beta^{-2/3}\sum_{\lambda=1}^{2}\int_0^{x_a}\varphi(r_{j\lambda}^{+})\,dx, \quad (4)$$

$$\langle Q_{abs}\rangle_{b.e.} = 2^{-1/3}\beta^{-2/3}\sum_{\lambda=1}^{2}\int_0^{x_b}[\varphi(r_{j\lambda}^{-}) - \varphi(\tilde{r}_{j\lambda}^{-})]\,dx, \quad (5)$$

where

$$\varphi(r_{j\lambda}) = (1-e^{-b})(1-r_{2\lambda})/(1-r_{1\lambda}e^{-b}), \quad (6)$$

and $r_{2\lambda}$ and $r_{1\lambda}$ are, respectively, the external and internal reflectivities for polarization λ, given by

$$r_{j\lambda} = |R_{j\lambda}|^2, \quad j,\lambda = 1,2; \quad R_{j\lambda} = (-1)^j(z_j - ue_\lambda)/(z + ue_\lambda); \quad (7)$$

$$z = \cos\theta, \quad u = N\cos\theta', \quad \sin\theta = N\sin\theta', \quad (8)$$

$$e_1 = 1, \quad e_2 = N^{-2}, \quad z_1 = z, \quad z_2 = \begin{cases} z \text{ for Eq. (3)} \\ z^* \text{ for Eqs. (4) and (5)}, \end{cases}$$

and

$$b = 4\beta\,\mathrm{Im}(N\cos\theta' + \theta'\sin\theta). \quad (9)$$

θ' is the *complex* angle of refraction corresponding to the angle of incidence θ. [(8) is just Snell's Law.] $r_{j\lambda}$ are the Fresnel reflectivities ($r_{2\lambda} = r_{1\lambda}$), and b is the damping exponent along a *complex* shortcut through the sphere. Thus (3) is an improved version of the geometrical-optic[1] result.

The terms (4) and (5) represent the contribution from the edge domain[3] (a.e. = above edge; b.e. = below edge); $r_{j\lambda}^{\pm}$ is obtained from $r_{j\lambda}$ by the substitution

$$z - z^{\pm} = -(2/\beta)^{1/3}e^{i\pi/6}\mathrm{Ai}'(\pm xe^{2i\pi/3})/\mathrm{Ai}(\pm xe^{2i\pi/3}), \quad (10)$$

where Ai is the Airy function, θ is related to x by

$$\sin\theta = 1 \pm 2^{-1/3}\beta^{-2/3}x \ (+ \text{ in a.e.}; - \text{ in b.e.}) \quad (11)$$

[with corresponding changes in the derived quantities (8) and (9)], and the limits of integration are

$$x_a = 2^{1/3}(n-1)\beta^{2/3}, \quad x_b = (\beta/2)^{2/3}. \quad (12)$$

Finally, in (5), $\tilde{r}_{j\lambda}^{-}$ is obtained from $r_{j\lambda}^{-}$ by the substitution

$$z^{-} \to (2/\beta)^{1/3}x^{1/2}. \quad (13)$$

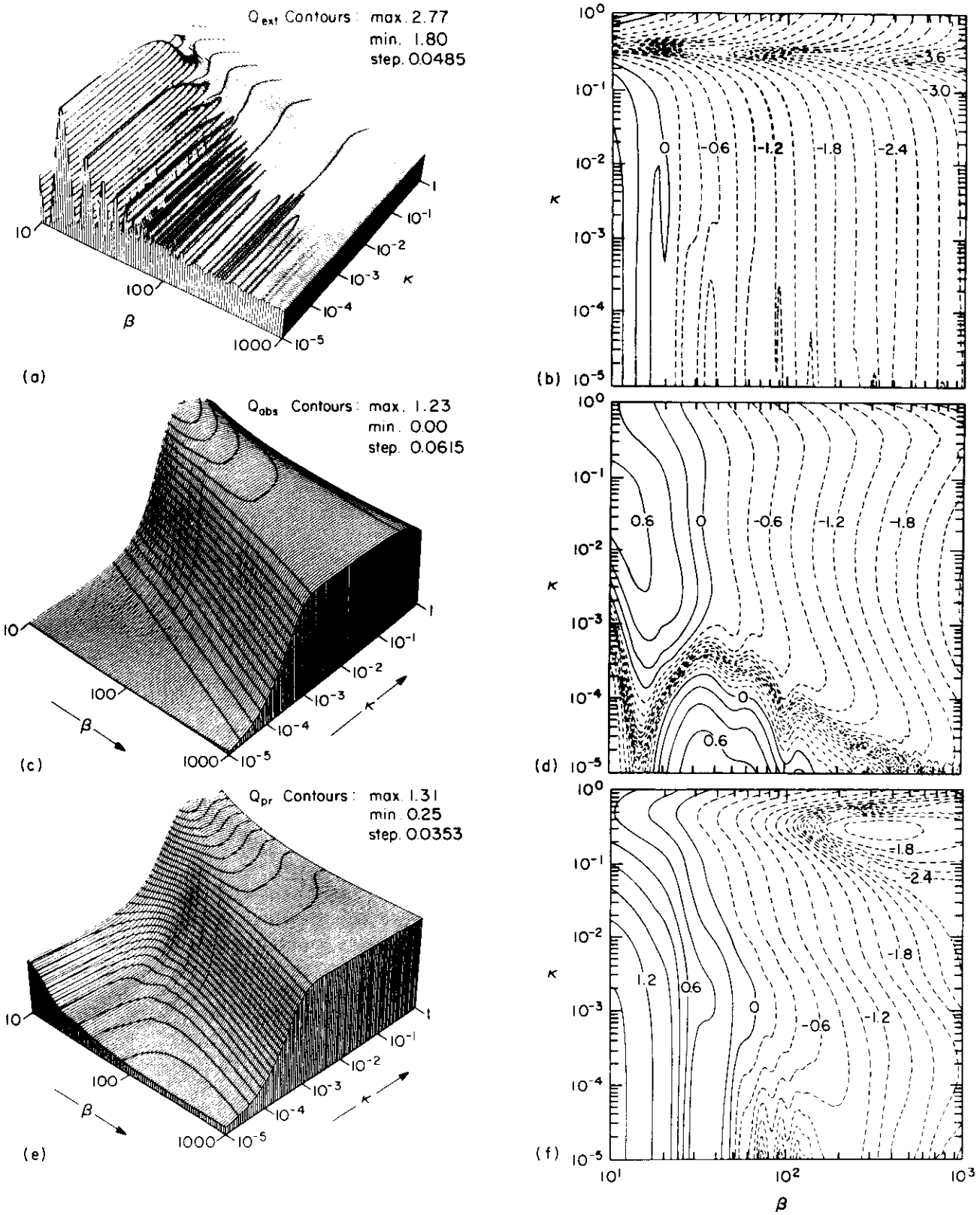

FIG. 1. (a) Three-dimensional plot of $\langle Q_{ext} \rangle$ for $n = 1.33$, $10^{-5} \leq \kappa \leq 1$, $10 \leq \beta \leq 10^3$. The numbers attached to surface represent values of $\langle Q_{ext} \rangle$. (b) Level curves for the logarithm of the percentage errors of the asymptotic approximation to $\langle Q_{ext} \rangle$. Negative values (errors $< 1\%$) are shown by dotted lines. (c) Same as (a) for $\langle Q_{abs} \rangle$. (d) Same as (b) for $\langle Q_{abs} \rangle$. (e) Same as (a) for $\langle Q_{pr} \rangle$. (f) Same as (b) for $\langle Q_{pr} \rangle$.

The average radiation-pressure efficiency is given by[6]

$$\langle Q_{pr}\rangle = 1 - \langle w_g\rangle_F - \langle w_g\rangle_{a.e.} - \langle w_g\rangle_{b.e.}, \tag{14}$$

$$\langle w_g\rangle_F = \mathrm{Re}\sum_{\lambda=1}^{2}\int_0^{\pi/2} d\theta \sin\theta\cos\theta e^{-2i\theta}[-|R_{2\lambda}|^2 + |1-(R_{2\lambda})^2|^2(1+f_2|R_{1\lambda}|^2 e^{-b})^{-1} f_2 e^{-b}], \tag{15}$$

$$\langle w_g\rangle_{a.e.} = 2^{-1/3}\beta^{-2/3}\,\mathrm{Re}\sum_{\lambda=1}^{2}\int_0^{x_a}(\rho_\lambda^{+} - \tau_\lambda^{+} + 1)\,dx, \tag{16}$$

$$\langle w_g\rangle_{b.e.} = 2^{-1/3}\beta^{-2/3}\,\mathrm{Re}\sum_{\lambda=1}^{2}\int_0^{x_b}[(\rho_\lambda^{-} - \hat{\rho}_\lambda^{-}) - (\tau_\lambda^{-} - \hat{\tau}_\lambda^{-})]\,dx, \tag{17}$$

where

$$\rho_\lambda = f_1(z) R_{2\lambda}^{*} R_{2\lambda}', \tag{18}$$

$$\tau_\lambda = f_1(z) f_2 e^{-b}(1+R_{1\lambda}^{*})(1+R_{1\lambda}')(1+R_{2\lambda}^{*})(1+R_{2\lambda}')(1+R_{1\lambda}^{*}R_{1\lambda}' f_2 e^{-b})^{-1}, \tag{19}$$

$$f_1(z) = (1+iz^{*})/(1-iz), \quad f_2 = e^{-2i\theta'}, \tag{20}$$

$$R_{j1}' = (f_j)^{-1}[N^2 z_j - u + (-1)^j iM^2](N^2 z + u + iM^2)^{-1}, \tag{21}$$

$$R_{j2}' = (f_j)^{-1}[(N^2+M^2)z_j - u + (-1)^j iM^2(1-uz_j)][(N^2+M^2)z + u + iM^2(1+uz)]^{-1}, \tag{22}$$

with $M^2 = N^2 - 1$. In all quantities with ($\pm$) upper indices, the substitutions (10) and (11) are understood. Finally, $\hat{\rho}_\lambda^{-}$ and $\hat{\tau}_\lambda^{-}$ are obtained from $\rho_\lambda^{-}, \tau_\lambda^{-}$ by the substitution

$$z^{-} \to (2/\beta)^{1/3}(\sqrt{x} + i/4x). \tag{23}$$

Again, (15) represents an improved version of the geometrical-optic[7] result, while (16) and (17) represent above-edge and below-edge corrections.

We have made detailed comparisons[6] between the exact Mie results (suitably averaged to eliminate the ripple[8]) and the above asymptotic approximations[9] over the ranges $10 \leq \beta \leq 5000$, $0 \leq \kappa \leq 1$, for $n = 1.10$, 1.33, 1.50, 1.90, and 2.50. Results for $n = 1.33$ and $10 \leq \beta \leq 1000$ are shown in Fig. 1.

Figure 1(a) is a three-dimensional plot of $\langle Q_{ext}\rangle$. The oscillations arise form interference between diffracted and transmitted light, and they are damped out as $\kappa\beta$ increases. Figure 1(b) shows level curves for the logarithm of the percentage error of approximation (1). Negative values (errors < 1%) are shown by dotted lines. Thus the relative error falls below 1% already at $\beta \gtrsim 15$, it is $\lesssim 0.1\%$ at $\beta \gtrsim 70$, $\lesssim 0.01\%$ at $\beta \gtrsim 200$, and $\lesssim 10^{-3}\%$ at $\beta \gtrsim 10^3$.

Figures 1(c) and 1(d) show similar plots for $\langle Q_{abs}\rangle$, and Figs. 1(e) and 1(f) for $\langle Q_{pr}\rangle$. The relative errors are somewhat greater than for $\langle Q_{ext}\rangle$ and are the worst for $\langle Q_{pr}\rangle$, where one must have $\beta \geq 90$ to achieve better than 1% error.

The accuracy improves not only as β increases, but also as n increases. Previously known approximations (based on geometrical optics and classical diffraction theory) have an accuracy that is almost independent of n and that only reaches 1% at $\beta = 1000$ and (0.2–0.5)% at $\beta = 5000$.

The computing time is reduced relative to exact Mie computations roughly by a factor of $O(\beta)$, and it is only about twice that for geometrical-optic approximations.

Besides the improvement to the geometrical-optic–type contributions, the main asymptotic corrections arise from the edge domain. Their functional form is quite similar to the geometrical-optic one, extended to complex angles of incidence and refraction. Thus, as was found in previous discussions,[3] the edge effects represent a kind of analytic continuation of ray optics to complex paths, where diffraction corresponds to barrier penetration. Similar interpretations have been suggested in atomic,[10] nuclear,[11] and particle[12] physics.

The National Center for Atmospheric Research is sponsored by the National Science Foundation.

[a]Permanent address: Instituto de Fisica, Universidade de São Paulo, 01000 São Paulo, Brazil.

[1]H. C. van de Hulst, *Light Scattering by Small Particles* (Wiley, New York, 1957).

[2]W. M. Irvine, J. Opt. Soc. Am. 55, 16 (1965).

[3]Cf. H. M. Nussenzveig, J. Opt. Soc. Am. 69, 1068 (1979), and references therein.

[4]H. M. Nussenzveig, J. Math. Phys. 10, 82, 125 (1969).

[5]V. Khare, Ph.D. thesis, University of Rochester, 1975 (unpublished).

[6]H. M. Nussenzveig and W. J. Wiscombe, to be published.

[7]P. J. Debye, Ann. Phys. 30, 57 (1909).

[8]The Mie computations were performed using algorithms of Wiscombe [Appl. Opt. 19, 1505 (1980)]. High-frequency ripple was removed from the Mie data by least-squares quartic spline fitting with knots every $\Delta\beta \sim 10$ for Q_{abs} and Q_{pr}, and by low-pass filtering for Q_{ext}.

[9]A fairly well-tested set of computer routines for calculating Eqs. (1), (2), and (14) is available from one of us (W.J.W.) upon request.

[10]J. N. L. Connor and W. Jakubetz, Mol. Phys. 35, 949 (1978); S. Bosanac, Mol. Phys. 35, 1057 (1978).

[11]R. C. Fuller and P. J. Moffa, Phys. C 15, 266 (1977).

[12]B. Schrempp and F. Schrempp, Phys. Lett. 70B, 88 (1977); Centre Européen de Recherches Nucléaires Report No. CERN-TH 2573, 1978 (to be published).